JASS Journal of Astronomy and Space Sciences

Pacific Equatorial Sea Surface Temperature Variation During the 2015 El Niño Period Observed by Advanced Very-High-Resolution Radiometer of NOAA Satellites

Seongsuk Lee, Yu Yi[†]

Department of Astronomy, Space Science and Geology, Chungnam National University, Daejeon 34134, Korea

El Niño is the largest fluctuation in the climate system, and it can lead to effects influencing humans all over the world. An El Niño occurs when sea surface temperatures in the central and eastern tropical Pacific Ocean become substantially higher than average. We investigated the change in sea surface temperature in the Pacific Ocean during the El Niño period of 2015 and 2016 using the advanced very-high-resolution radiometer (AVHRR) of NOAA Satellites. We calculated anomalies of the Pacific equatorial sea surface temperature for the normal period of 1981–2010 to identify the variation of the 2015 El Niño and warm water area. Generally, the warm water in the western tropical Pacific Ocean shifts eastward along the equator toward the coast of South America during an El Niño period. However, we identified an additional warm water region in the Niño 1+2 and Peru coastal area. This indicates that there are other factors that increase the sea surface temperature. In the future, we will study the heat coming from the bottom of the sea to understand the origin of the heat transport of the Pacific Ocean.

Keywords: sea surface temperature, El Niño, advanced very-high-resolution radiometer

1. INTRODUCTION

Sea surface temperature (SST) is an important factor for understanding the climate system. SST analysis has been used to monitor and predict climate by converting irregular SST grid data to a regular grid (Smith & Reynolds 2003). The SST analysis data by the National Oceanic and Atmospheric Administration (NOAA) (Reynolds & Smith 1994; Reynolds et al. 2002) use infrared satellite data from the advanced very-high-resolution radiometer (AVHRR) and in situ data from ships and buoys on a 1° spatial grid from November 1981 to present. The new analysis SST data were developed using optimum interpolation (OI) at a spatial grid resolution of 0.25° (Reynolds et al. 2007).

El Niño is a large-scale oceanic warming phenomenon in the tropical Pacific Ocean that occurs on average every two to seven years. Many studies have explained this event as interactions between the tropical Pacific Ocean and the atmosphere. Bjerknes (1969) hypothesized a positive ocean–atmosphere feedback involving the Walker circulation. When the Pacific Ocean is under the normal condition, warm water accumulates west of the date line because the trade winds push water to the west. Air in the tropical western Pacific rises and then flows eastward. This is known as Walker circulation. The water flow is from east to west in the normal condition. During the El Niño period, a positive SST anomaly in the equatorial eastern Pacific decreases the east–west SST gradient and the strength of the Walker circulation (Gill 1980; Lindzen & Nigam 1987). The trade winds weaken, thus changing the ocean circulation and SST anomaly. This feedback produces the equatorial Pacific area warm condition (Philander 1981). The water flow is from west to east during the El Niño period (Bjerknes 1969; Philander 1990; McCreary Jr. & Anderson 1991; Neelin et al. 1998).

The Nino 1+2, Nino 3, Nino 3.4, and Nino 4 SST indices are used to monitor the tropical Pacific and are calculated based on SST anomalies averaged across a respective region (Rasmusson & Carpenter 1982). El Niño has been quantified

by several indices as corresponding to times when SST anomalies exceed 0.5 °C in the Nino 3 region using a 5-month running average or 0.4 °C in the Nino 3.4 region using a 3-month running average (Trenberth 1997; Trenberth & David 2001).

2. DATA AND METHOD

Specifically, for the Pacific equatorial region, we used the NOAA OI SST V2 product (Reynolds et al. 2007), provided by the NOAA Earth System Research Laboratory (ESRL) Physical Sciences Division (http://www.esrl.noaa.gov/psd/data), to show the variation of the 2015 El Niño events. NOAA OI SST provides an alternate database of SST data that is a spatial grid resolution of 0.25° latitude × 0.25° longitude global grid (1,440 × 720) with a temporal resolution of 1 day.

We used a high-resolution OI of AVHRR infrared satellite SST data from a series of National Oceanic and Atmospheric Administration (NOAA) satellites. The NOAA Satellite, a series satellite, provides Earth's observation data to monitor global environment and understand our dynamic Earth. Table 1 show NOAA series satellites and AVHRR sensor type. The AVHRR is a radiation-detection imager that has four- or five-channel scanners and can be used remotely for determining cloud cover and surface conditions. They

sense in the visible, thermal infrared, and infrared portions of the electromagnetic spectrum. The AVHRR dataset has been used in many fields. In the case of visible observation, the scanners have been used to monitor sea ice and snow or vegetation. The infrared observation can be used to measure sea surface temperature. Thus, the datasets from AVHRR can be used effectively to study global environmental change. We have summarized the characteristics and use of the AVHRR sensor (Table 2).

The SST data by AVHRR are available from late 1981 to 2016 and operational AVHRR data are provided for 2017 onward. There are two types of daily OISST (Reynolds et al. 2007). One product is the AVHRR-only product, which uses AVHRR data and in-situ data from ships and buoys. The other product (AVHRR+AMSR) uses AVHRR, advanced microwave scanning radiometer (AMSR), and in situ data.

In this paper, we selected the AVHRR-only dataset because this dataset includes consistent long-term collections over the world (Banzon et al. 2016). We averaged over thirty years (1982–2011) from the AVHRR-only dataset to obtain an average at 0.25° spatial grid points for one year. Then, we computed the SST anomaly from the selected base period (1982–2011). We identified the variation of SST during the 2015 El Niño period from the calculated SST anomaly data.

We also used the SST index data in the Nino 1+2, Nino 3, and Nino 4 regions to reveal warm water regions in the sea surface during the 2015 El Niño period. The Niño SST index data were calculated from the Hadley Centre sea ice and sea surface temperature data set (HadISST) from 1870 to Mar 2018 (Rayner et al. 2003). The Niño 1+2 index is the averaged SST anomalies within the region of 0–10°S and 90–80°W, the Niño 3 index is the averaged SST anomalies within 5°S–5°N and 150–90°W, and the Niño 4 index is the averaged SST anomalies within 5°S–5°N and 160°E–150°W.

3. RESULTS

We investigated the strong SST anomaly during the 2015 El Niño period to show the warm sea surface regions in the tropical sea surface area. Fig. 1 shows the sea surface temperature anomalies for June 2015 in the Niño 1+2, Niño

Table 1. Launch, service dates and AVHRR sensor type of the NOAA Satellites

Satellite name	Launch date	Service starts	Service ends	AVHRR
TIROS-N	13 Oct 1978	19 Oct 1978	30 Jan 1980	AVHRR/1
NOAA-6	27 Jun 1979	27 Jun 1979	16 Nov 1986	AVHRR/1
NOAA-7	23 Jun 1981	24 Aug 1981	07 Jun 1986	AVHRR/2
NOAA-8	28 Mar 1983	03 May 1983	31 Oct 1985	AVHRR/1
NOAA-9	12 Dec 1984	25 Feb 1985	11 May 1994	AVHRR/2
NOAA-10	17 Sep 1986	17 Nov 1986	17 Sep 1991	AVHRR/1
NOAA-11	24 Sep 1988	08 Nov 1988	13 Sep 1994	AVHRR/2
NOAA-12	13 May 1991	14 May 1991	15 Dec 1994	AVHRR/2
NOAA-14	30 Dec 1994	30 Dec 1994	23 May 2007	AVHRR/2
NOAA-15	13 May 1998	13 May 1998	Present	AVHRR/3
NOAA-16	21 Sep 2000	21 Sep 2000	09 Jun 2014	AVHRR/3
NOAA-17	24 Jun 2002	24 Jun 2002	10 Apr 2013	AVHRR/3
NOAA-18	20 May 2005	30 Aug 2005	Present	AVHRR/3
NOAA-19	06 Feb 2009	02 Jun 2009	Present	AVHRR/3

Table 2. Spectral characteristics and use of AVHRR sensors

Channel	TIROS-N	NOAA-6,8,10	NOAA-7,9,11,12,14	NOAA-15,16,17,18,19	Typical use
1	0.550- 0.90 μm	0.580- 0.68 μm	0.580- 0.68 μm	0.50 - 0.68 μm	Day time cloud and surface mapping
2	0.725- 1.10 μm	0.725- 1.10 μm	0.725- 1.10 μm	0.725-1.0 μm	Land-water boundaries
3A	-	-	-	1.58-1.64 μm	Snow and ice detection
3B	3.550- 3.93 μm	3.550- 3.93 μm	3.550- 3.93 μm	3.55-3.93 μm	Night cloud mapping, sea surface temperature
4	10.50-11.50 μm	10.50-11.50 μm	10.30-11.30 μm	10.3-11.3 μm	Night cloud mapping, sea surface temperature
5	Ch4 rep.	Ch4 rep.	11.50-12.50 μm	11.5-12.5 μm	Sea surface temperature

3, and Niño 4 regions when the El Niño warm phase began to spread around the equatorial region. The formation of El Niño is generally explained by a weakening or reversal from normal of the direction of the trade winds, which allows warm sea surface water to move eastward. In addition to the warm water coming from the west, we identified a warm water region in the Niño 1+2 and coastal Peru area, as shown in Fig. 1. We investigated the SST mean anomalies in the Niño 1+2, 3, and 4 regions to show the long-term variation of the sea surface temperature anomalies (Fig. 2). We found that the Niño 1+2 region has had a higher anomaly value than the Niño 3 or Niño 4 regions, as shown in Figs. 2 and 3. Fig. 4 shows a series of SST anomaly maps from January 2015 to June 2016. We used high-resolution satellite observations data for the SST maps, the NOAA OI SST V2 product (Reynolds et al. 2007), to show the warm water region of the El Niño event where water could be rising upward from below the Niño 1+2 region. The SST anomaly for the El Niño condition tends to peak in December, and the peak of the 2015 El Niño occurred in the winter of 2015–16 (Fig. 4). During the El Niño event, there was warm water in the Niño 1+2 and Peru coastal area from June 2015 to March 2016.

4. SUMMARY AND DISCUSSION

Normally, the movement of warm water in the western tropical Pacific Ocean is eastward during an El Niño period. We identified an additional warm water area in the Niño 1+2 region and the Peru coastal area using the high-resolution sea surface temperature dataset from the AVHRR and the Niño index supported by HadISST. The study of Lee & Yi (2016) suggested sources of heat from the bottom of the sea as a cause of melting of Arctic sea ice. We believe that
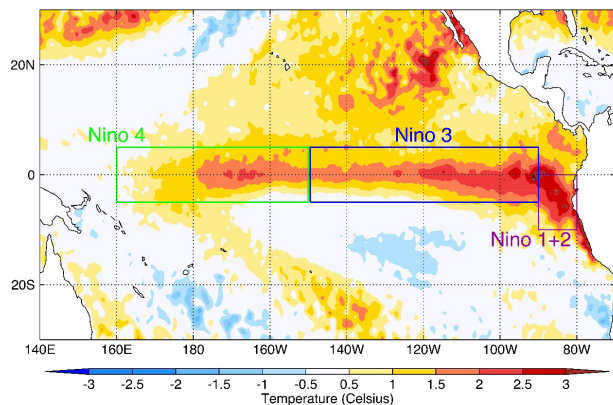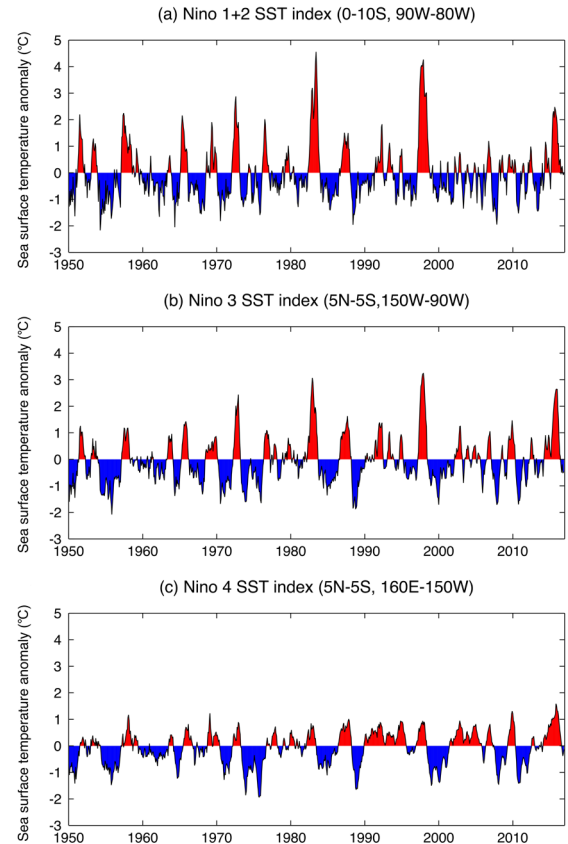

Fig. 2. SST indices for the Niño 1+2, Niño 3, and Niño 4 regions (a) SST anomaly in the Niño 1+2 region of averaged SST from 0–10°S and 90–80°W (b) SST anomaly in the Niño 3 region of averaged SST from 5°S–5°N and 150–90°W (c) SST anomaly in the Niño 4 region of averaged SST from 5°S–5°N and 160°E–150°W.

the cause of this study are also applicable to the equatorial region. Therefore, to understand the mechanism of El Niño better, it is necessary to check both the surface condition and also the submarine condition.
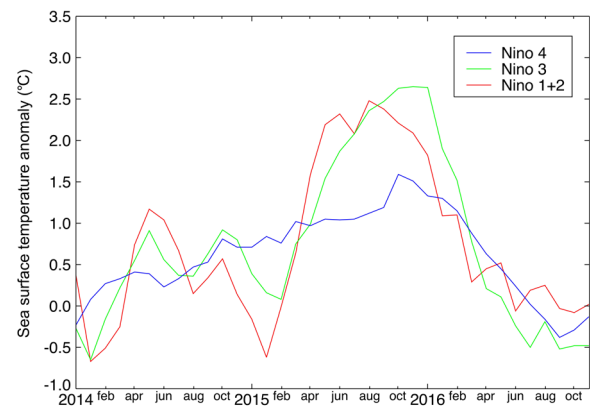

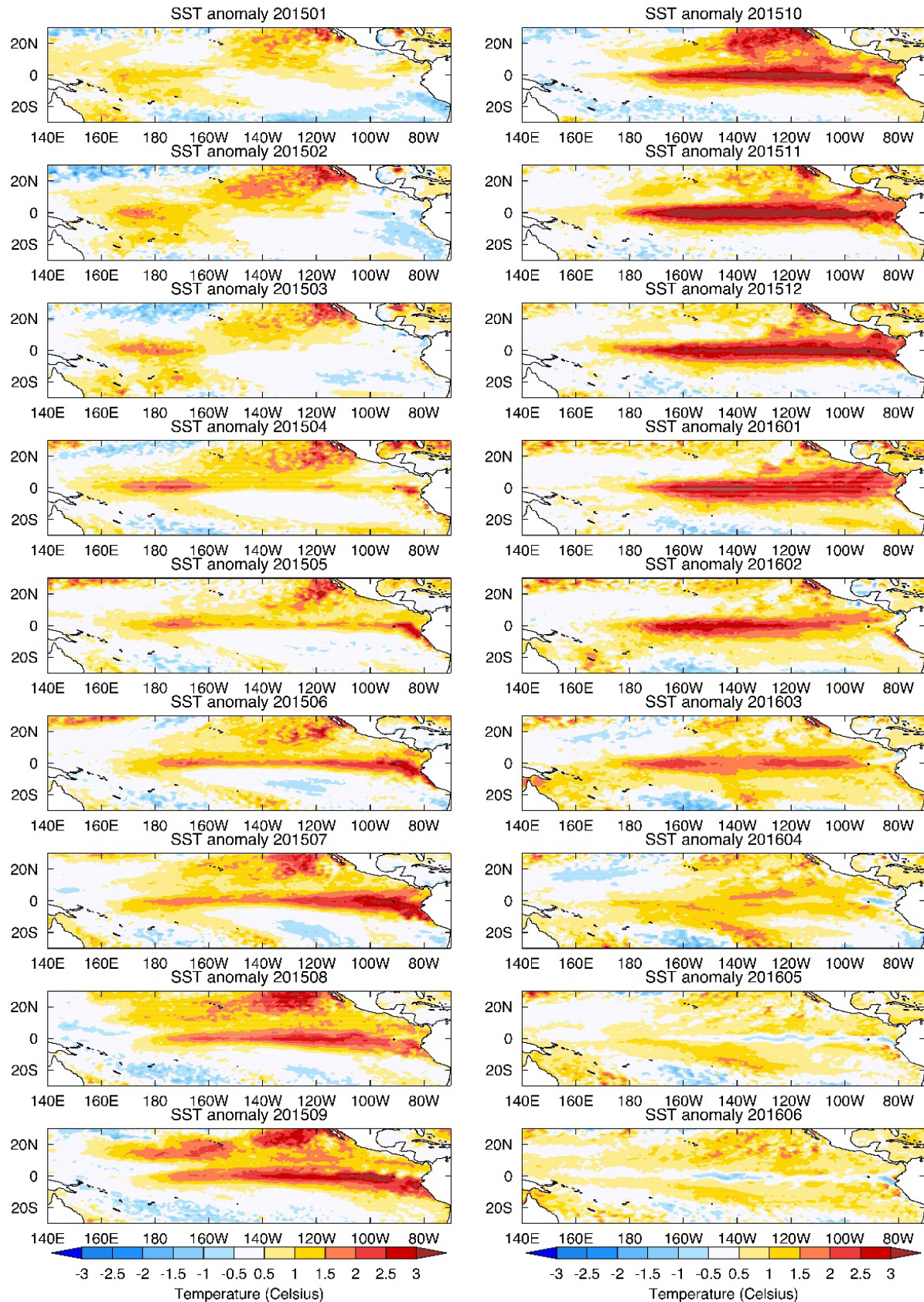**Fig. 1.** SST anomaly in the Niño 1+2, Niño 3, and Niño 4 regions for June 2015 relative to the monthly mean of 1982–2011.

Fig. 3. SST anomalies of the Niño 1+2, Niño 3, and Niño 4 regions during the 2015 El Niño period.

Fig. 4. SST anomalies maps from January 2015 to June 2016 (30°S–30°N, 140°E–70°W).

ACKNOWLEDGMENTS

REFERENCES

Banzon V, Smith TM, Chin TM, Liu C, Hankins W, A long-term record of blended satellite and in situ sea-surface temperature for climate monitoring, modeling and environmental studies, Earth Syst. Sci. Data 8, 165-176 (2016). https://doi.org/10.5194/essd-8-165-2016

Bjerknes J, Atmospheric teleconnections from the equatorial Pacific, Mon. Weather. Rev. 97, 163-172 (1969). https://doi.org/10.1175/1520-0493(1969)097<0163:ATFTEP>2.3.CO;2

Gill AE, Some simple solutions for heat-induced tropical circulation, Q. J. R. Meteorol. Soc. 106, 447-462 (1980). https://doi.org/10.1002/qj.49710644905

Lee S, Yi Y, Abnormal winter melting of the Arctic sea ice cap observed by the spaceborne passive microwave sensors, J. Astron. Space Sci. 33, 305-311 (2016). https://doi.org/10.5140/JASS.2016.33.4.305

Lindzen RS, Nigam S, On the role of sea surface temperature gradients in forcing low-level winds and convergence in the Tropics, J. Atmos. Sci. 44, 2418-2436 (1987). https://doi.org/10.1175/1520-0649(1987)044<2418:OTROSS>2.0.CO;2

McCreary Jr. JP, Anderson DLT, An overview of coupled ocean-atmosphere models of El Niño and the southern oscillation, J. Geophys. Res. 96, 3125-3150 (1991). https://doi.org/10.1029/90JC01979

Neelin JD, Battisti DS, Hirst AC, Jin FF, Wakata Y, et al., ENSO theory, J. Geophys. Res. 103, 14262-14290 (1998). https://doi.org/10.1029/97JC03424

Philander SGH, The response of equatorial oceans to a relaxation of the trade winds, J. Phys. Oceanogr. 11, 176-189 (1981). https://doi.org/10.1175/1520-0485(1981)011<0176:TROEOT>2.0.CO;2

Philander SGH, El Niño, La Niña and the southern oscillation (Academic Press, San Diego, 1990).

Rasmusson EM, Carpenter TH, Variations in tropical sea surface temperature and surface wind fields associated with the southern oscillation/El Niño, Mon. Weather. Rev. 110, 354-384 (1982). https://doi.org/10.1175/1520-0493(1982)110<0354:VITSST>2.0.CO;2

Rayner NA, Parker DE, Horton EB, Folland CK, Alexander LV, et al., Global analyses of sea surface temperature, sea ice, and night marine air temperature since the late nineteenth century, J. Geophys. Res. 108, D14 (2003). https://doi.org/10.1029/2002JD002670

Reynolds RW, Smith TM, Improved global sea surface temperature analyses using optimum interpolation, J. Clim. 7, 929-948 (1994). https://doi.org/10.1175/1520-0442(1994)007<0929:IGSSTA>2.0.CO;2

Reynolds RW, Rayner NA, Smith TM, Stokes DC, Wang W, An improved in situ and satellite SST analysis for climate, J. Clim. 15, 1609-1625 (2002). https://doi.org/10.1175/1520-0442(2002)015<1609:AIISAS>2.0.CO;2

Reynolds RW, Smith TM, Liu C, Chelton DB, Casey KS, et al., Daily high-resolution blended analyses for sea surface temperature, J. Clim. 20, 5473-5496 (2007). https://doi.org/10.1175/2007JCLI1824.1

Smith TM, Reynolds RW, Extended reconstruction of global sea surface temperatures based on COADS data (1854-1997), J. Clim. 16, 1495-1510 (2003). https://doi.org/10.1175/1520-0442(2003)016<1495:EROGSS>2.0.CO;2

Trenberth KE, The definition of El Niño, Bull. Am. Meteorol. Soc. 78, 2771-2777 (1997). https://doi.org/10.1175/1520-0477(1997)078<2771:TDOENO>2.0.CO;2

Trenberth KE, Stepaniak DP, Indices of El Niño evolution, J. Clim. 14, 1697-1701 (2001). https://doi.org/10.1175/1520-0442(2001)014<1697:LIOENO>2.0.CO;2